JOURNAL OF VIROLOGY, Nov. 2006, p. 10372–10381 Vol. 80, No. 21
0022-538X/06/$08.00+0 doi:10.1128/JVI.00809-06

Pathogenesis of a Genogroup II Human Norovirus in Gnotobiotic Pigs

Sonia Cheetham,[1] Menira Souza,[1] Tea Meulia,[2] Sheila Grimes,[3] Myung Guk Han,[1] and Linda J. Saif[1]*

Food Animal Health Research Program, Ohio Agricultural Research and Development Center, Department of Veterinary Preventive Medicine, The Ohio State University, Wooster, Ohio 44691[1]; Molecular and Cellular Imaging Center, Ohio Agricultural Research and Development Center, Wooster, Ohio[2]; and Animal Disease Diagnostic Laboratory, Ohio Department of Agriculture, Reynoldsburg, Ohio[3]

Received 19 April 2006/Accepted 3 August 2006

We evaluated the gnotobiotic (Gn) pig as a model to study the pathogenesis of human norovirus (HuNoV) and to determine the target cells for viral replication. Sixty-five Gn pigs were inoculated with fecal filtrates of the NoV/GII/4/HS66/2001/US strain or with pig-passaged intestinal contents (IC) and euthanized acutely (n = 43) or after convalescence (n = 22). Age-matched Gn piglets (n = 14) served as mock-inoculated controls. Seventy-four percent (48/65) of the inoculated animals developed mild diarrhea compared to 0 of 14 controls. Pigs from postinoculation days (PID) 1 to 4 tested positive for HuNoV by reverse transcription-PCR of rectal swab fluids (29/65) and IC (9/43) and by antigen (Ag) enzyme-linked immunosorbent assay (ELISA) using antiserum to virus-like particles of HuNoV GII/4. No control pigs were positive. Histopathologic examination showed mild lesions in the proximal small intestine of only one pig (1/7). Seroconversion after PID 21 was detected by antibody ELISA in 13 of 22 virus-inoculated pigs (titers, 1:20 to 1:200) but not in controls. Immunofluorescent microscopy using a monoclonal antibody to HuNoV GII capsid revealed patchy infection of duodenal and jejunal enterocytes of 18 of 31 HuNoV-inoculated pigs with a few stained cells in the ileum and no immunofluorescence (IF) in mock-inoculated controls. Immunofluorescent detection of the viral nonstructural N-terminal protein antigen in enterocytes confirmed translation. Transmission electron microscopy of intestines from HuNoV-inoculated pigs showed disrupted enterocytes, with cytoplasmic membrane vesicles containing calicivirus-like particles of 25 to 40 nm in diameter. In summary, serial passage of HuNoV in pigs, with occurrence of mild diarrhea and shedding, and immunofluorescent detection of the HuNoV structural and nonstructural proteins in enterocytes confirm HuNoV replication in Gn pigs.

Human noroviruses (HuNoVs) are a major cause of foodborne gastroenteritis worldwide. Because they do not grow in cell culture and there is no animal model for HuNoVs, pathogenesis studies have been hampered. Thus, little is known about their replication strategies or induction of neutralizing antibodies.

The limited information on their pathogenesis is from human volunteer studies of HuNoV infections in which villus atrophy in duodenal biopsies and presence of malabsorptive diarrhea were described (1, 7, 8). No information is available on lesions in other portions of the intestines of these volunteers (9). Intestinal transplant pediatric patients that were diagnosed with HuNoV infection developed secretory or osmotic diarrhea (19, 20, 31). These patients had prolonged diarrhea (17 to 326 days) due to immunosuppressive therapy. The detection of HuNoV RNA and the clinical symptoms remitted after reduction of the immunosuppressive therapy. Usually in exposed individuals, histologic lesions correlate with diarrhea, but in one report, lesions in volunteers who did not show clinical symptoms were described (42). There are also numerous reports of asymptomatic individuals who were infected with HuNoVs and shed virus in the feces (11, 28).

* Corresponding author. Mailing address: Food Animal Health Research Program, Ohio Agricultural Research and Development Center, The Ohio State University, 1680 Madison Avenue, Wooster, OH 44691. Phone: (330) 263-3744. Fax: (330) 263-3677. E-mail: saif.2@osu.edu.

Most past attempts to study these viruses in an animal model may have failed because (i) the human strains that were used were not closely related to the host animal NoV strains, (ii) sensitive detection techniques were lacking, and finally (iii) the role of histo-blood group antigen (HBGA) phenotypes in differential susceptibility of the host was unrecognized. Our goal was to adapt a HuNoV strain to replicate in the gnotobiotic (Gn) pig to develop an animal model for the study of HuNoV pathogenesis. Gnotobiotic pigs are good models for human enteric diseases (40) because pigs resemble humans in their gastrointestinal anatomy, physiology, and immune responses. The Gn pigs are immunocompetent at birth, but they lack maternal antibodies and previous or ongoing exposure to microbial agents, including caliciviruses.

Recently, viral RNA genetically similar to that of human NoV GII (65 to 71% amino acid sequence identity in the capsid gene) was detected in pigs in Japan (46, 47) and Europe (22, 48). In U.S. swine, our laboratory detected both viral RNA and virus particles similar to GII HuNoV (70% sequence identity in the capsid region) which were infectious for Gn pigs (50). Our approach to infect Gn pigs with a HuNoV was to use a GII strain that is closely related genetically to the identified GII porcine NoVs and that has a broad HBGA binding pattern because little information or reagents are available for pig HBGA. Additionally, we used sensitive assays and reagents including reverse transcription (RT)-PCR to detect fecal shedding, virus-like particles (VLPs) for serological assays, and antisera to these VLPs for antigen enzyme-linked immunosor-

bent assay (ELISA) to increase the sensitivity of virus detection in the exposed Gn pigs.

In this study, Gn pigs were inoculated orally ($n = 63$) or intravenously ($n = 2$) with a HuNoV GII/4 strain and infection was monitored by the presence of diarrhea, fecal virus shedding, infected cells in intestinal tissues, and seroconversion. Age-matched, mock-inoculated Gn pigs ($n = 14$) served as controls. Most virus-inoculated pigs developed diarrhea, and nearly half shed virus in the feces or seroconverted. In addition, viral antigen and calicivirus-like particles were detected in the cytoplasm of intestinal epithelial cells of some inoculated Gn pigs by immunofluorescent staining to the capsid and nonstructural N-terminal protein antigens and electron microscopy, respectively. These data suggest that HuNoV replicated in intestinal epithelial cells and was shed in the feces of at least some virus-inoculated pigs.

MATERIALS AND METHODS

Experimental animals and inocula. Gnotobiotic pigs were delivered and maintained as previously described (29). All animal protocols used in this study were approved by the Institutional Laboratory Animal Care and Use Committee. The original human fecal sample identified as the NoV/GII/4/HS66/2001/US (HS66) strain was collected from a child with diarrhea at Children's Hospital in Columbus, Ohio, and was kindly provided by J. Hughes, The Ohio State University. As determined by the medical history, the clinical signs of acute gastroenteritis, and the immune electron microscopy (IEM) results, other viruses such as human immunodeficiency virus, hepatitis virus, and rotaviruses were not present. We used the inoculum as a single aliquoted pool throughout our study. The viral RNA titer of the original sample was semiquantified by real-time RT-PCR (S. Cheetham, M. Souza, and L. J. Saif, unpublished data) as approximately 5.4×10^6 genomic equivalents (GE)/ml. The original human fecal sample was designated passage 0 (P0). P1 was an RT-PCR-positive pool of intestinal contents (IC) from Gn pigs inoculated with P0, and P2 was the RT-PCR-positive IC of a Gn pig inoculated with P1. Two additional pigs were orally inoculated with a fecal filtrate of P0-inactivated virus prepared by incubation with 0.01 M binary ethylenimine for 18 h at 37°C with continuous agitation as previously described (55). Sodium thiosulfate (1 M) was added to a final concentration of 10% to inactivate the binary ethylenimine, followed by dialysis with a cassette (Pierce Biotechnology, Rockford, IL). Sixty-five Gn piglets were inoculated with 5 ml of diluted HS66 strain stool filtrate from the original human sample or derivatives from it after serial passages in Gn pigs. Briefly, the original human fecal sample was diluted 1:10 in minimal essential medium (MEM) (Gibco, Invitrogen, Carlsbad, CA), vortexed for 1 min, centrifuged at $3,000 \times g$ for 20 min to clarify, and passed through 0.8- and then 0.2-μm-pore-size syringe filters. The P1 and P2 inocula were diluted and clarified similarly but not filtered because the intestinal contents of the Gn pigs were sterile. Pigs were divided into groups according to the inocula (P0, P1, and P2). Group A pigs ($n = 37$) were orally inoculated with P0 except for one pig that was inoculated intravenously. Group B pigs ($n = 18$) were orally inoculated with P1 except for one pig that was inoculated intravenously. Group C pigs ($n = 10$) were orally inoculated with P2. Fourteen age-matched piglets were orally inoculated with MEM and served as mock-inoculated controls. Twelve of these pigs (six from group A, three from group B, and three controls) received oral dexamethasone (1 mg/kg of body weight/day) for 10 days to mimic the immunosuppression in transplanted individuals (19, 20, 31).

Daily rectal swabs were collected from 0 to 10 postinoculation days (PID), and diarrhea was assessed (scores: 0, normal; 1, creamy; 2, pasty; and 3, watery). Pigs with samples scores 2 and 3 were considered to have diarrhea. Two researchers scored the samples from all the Gn pigs. Pigs were euthanized during the acute phase (PID 1 to 5) ($n = 51$; 43 virus inoculated and 8 controls), and intestinal tissues were harvested for histopathologic examination ($n = 9$), immunofluorescent microscopy ($n = 39$), and transmission electron microscopy (TEM) ($n = 13$). A subset of 10 pigs (8 virus inoculated and 2 controls) were bled daily for 10 days to evaluate the presence of viremia. Some pigs ($n = 28$; 22 virus inoculated and 6 controls) were kept until PID 21 to evaluate seroconversion, the duration of viral shedding, and diarrhea.

RT-PCR, internal control, and real-time RT-PCR. The RNA extraction from rectal swab fluids, 1:20 dilutions of IC, and 1:50 dilutions of serum were performed using TRIZOL LS (Invitrogen) as directed by the manufacturer. A one-step RT-PCR assay was conducted using the Mon 431/433 primers (36) directed to the RNA-dependent RNA polymerase (RdRp) region of HuNoV GII. The RT-PCR conditions were 42°C for 60 min, 94°C for 3 min, and 40 cycles of 94°C for 30 s, 50°C for 30 s, and 72°C for 30 s, with a final extension of 72°C for 10 min. Amplicons were visualized by electrophoresis in 2% agarose gels stained with ethidium bromide under UV light. The product specificity was confirmed by sequencing or microplate hybridization as described by Wang et al. (49) using a probe specific for the HS66 strain (PmonHS66, 5′-CTTGCTAATT TTGCTGTAGAATGATGGGCCGTGGA-3′). Negative controls for RNA extraction and RT-PCR assays (mock-inoculated pigs and water) were included in each assay. To detect RT-PCR inhibitors and overcome possible false-negative results often encountered with fecal samples, we engineered a competitive internal control. Briefly, sequences complementary to primer pairs P289/290 (18) and Mon 431/433 were added by RT-PCR to a β-2 microglobulin DNA sequence at the 3′ and 5′ ends and subsequently cloned into a plasmid (pCR2.1 vector; Invitrogen). This plasmid served as template for in vitro transcription (Promega, Madison, WI) of the internal control RNA. The specific HuNoV product had a size of 211 bp, whereas the internal control was 320 bp long. The RNA samples that showed inhibition were diluted in diethyl pyrocarbonate-treated water and retested as described previously (49).

One-step, real-time RT-PCR was standardized using serial dilutions of known concentrations of the internal control (described above). The internal control was used as an external amplicon to generate a noncompetitive standard curve with Mon 431/433 primers using SYBR green I (Roche, Indianapolis, IN) (Cheetham, Souza, and Saif, unpublished) with the same cycling conditions as described earlier for viral shedding detection.

Cloning and expression of HS66 capsid gene and production of VLPs. ELISAs were initially standardized using VLPs and hyperimmune antisera to a strain (MD145, GII/4) kindly provided by K. Green (NIAID, NIH, Bethesda, MD). The MD145 strain is from the same genotype as HS66 and shares 95.9% and 94.4% amino acid and nucleotide identity, respectively, in the ORF2 encoding the capsid protein. Subsequently, we cloned the capsid gene of HS66 and generated a recombinant baculovirus clone expressing the HS66 capsid gene. A baculovirus expression system was used to produce HS66 NoV VLPs using *Spodoptera frugiperda* (Sf9) insect cells (16). First, the capsid gene was amplified by RT-PCR from the original fecal sample RNA using forward primer HS66ORF2f (5′-GGCTCCCAGTTTTGTGAATG-3′) and reverse primer HS66ORF2r (5′-AACCAAGTCCAGAGCCAAGG-3′) with the following reaction characteristics: annealing temperature of 52°C and extension time of 2 min. The amplicon was first cloned into a pCR2.1 vector (Invitrogen) and then subcloned into a baculovirus transfer vector, pBlueBac4.5 (Invitrogen), using the EcoRI restriction enzyme site. The recombinant plasmid that contained the full-length capsid gene in the correct orientation and the linearized wild-type baculovirus DNA were used to cotransfect Sf9 cells. After confirming the recombinant plaques by PCR and three rounds of plaque purification, we produced a recombinant baculovirus stock containing the capsid gene. For VLP production, Sf9 cells were infected with the recombinant baculovirus at a multiplicity of infection of 10 and harvested at PID 7 to 10. The supernatants were collected and centrifuged at $3,000 \times g$ for 30 min to remove cells. With the VLPs still in the liquid phase, concentration was performed by ultracentrifugation at $110,000 \times g$ for 2 h at 4°C through a 40% sucrose cushion. The pellet containing the VLPs was resuspended in TNC buffer (10 mM Tris HCl, 140 mM NaCl, 10 mM $CaCl_2$, pH 7.4), and the VLPs were purified by CsCl gradient ultracentrifugation at $150,000 \times g$ at 4°C for 18 h. The visible VLP bands were collected by aspiration, diluted in TNC buffer, and repelleted by ultracentrifugation at $110,000 \times g$ at 4°C for 2 h to remove the CsCl. The self-assembled VLPs were tested for integrity and reactivity by IEM, antigen ELISA, and Western blotting. The protein concentration was measured using the Bradford quantification method (Bio-Rad, Hercules, CA).

Production of hyperimmune serum. A guinea pig was first immunized with HS66 VLPs (500 μg) mixed with Freund's complete adjuvant via subcutaneous injection followed by four booster injections of the same dose in Freund's incomplete adjuvant with a 10-day interval between doses. The immunoglobulin G (IgG) VLP-specific antibody ELISA titer of the hyperimmune antiserum was >10,000.

Antibody ELISA. The antibody ELISA was adapted from previously described procedures (15) with modifications. We used CsCl-purified HuNoV GII/4 MD145 VLPs or HuNoV GII/4 HS66 VLPs to coat 96-well microtiter plates (Nalge Nunc, Rochester, NY) at a final concentration of 2.5 μg/ml (100 μl/well) in coating buffer (0.05 M carbonate buffer, pH 9.6). Plates were incubated at 4°C overnight. Blocking was performed with 2% skim milk in phosphate-buffered saline (PBS) buffer (10 mM potassium phosphate, 150 mM NaCl, pH 7.4) at 37°C for 1 h. Fourfold serial dilutions, beginning at 1:10, of the pig paired serum

samples were added to wells, and the plates were incubated for 3 h at 37°C. A mouse monoclonal antibody to pig IgG (3H7D7) (34) conjugated to biotin was added to the plates (1:10,000), and plates were incubated for 1 h at 37°C, followed by addition of streptavidin-horseradish peroxide (HRP) (1:2,000) and incubated at 37°C for 1 h. The assay samples were developed with tetramethylbenzidine (KPL, Gaithersburg, MD), incubated for 15 to 20 min at room temperature (Rt), and stopped with HCl (0.1 M). Plates were washed four times between each step with PBS containing 0.5% Tween 20. Serum from mock-inoculated control pigs and unrelated rotavirus VLP (55)-coated wells were used as negative controls. Positive samples were those with an absorbance equal to or greater than the cutoff which was determined as the mean of the antibody-negative control wells plus three times the standard deviation. For the paired sera (preinoculation and PID 21), seroconversion was defined as a fourfold increase in the convalescent-phase serum titer compared to the preinoculation serum sample.

The immunostaining of fixed recombinant baculovirus-infected Sf9 cell assay was performed as previously described (56) as another way to detect HuNoV-specific antibodies. Briefly, nearly confluent monolayers of Sf9 cells in 96-well plates were infected with the recombinant baculovirus expressing the HS66 capsid protein at a multiplicity of infection of 5 and incubated at 27°C for 5 days. Medium was aspirated from the wells, and the plates were then air dried and fixed with 3.7% formaldehyde for 30 min at Rt. Cells were permeabilized with 1% Triton X-100 (Sigma, St. Lois, MO) in TNC buffer for 5 min at Rt and then rinsed with PBS (pH 7.4). Serial twofold dilutions of pig serum samples beginning at 1:10 were added to the wells and incubated for 2 h at 37°C. The plates were rinsed in PBS, goat anti-pig IgG antibody conjugated to HRP was added, and the plates were incubated for 2 h at 37°C and developed with 3-amino-9-ethylcarbazole substrate (Vector Labs, Burlingame, CA). The antibody titer was defined as the reciprocal of the highest serum dilution at which a positive cell could be detected using light microscopy.

Antigen ELISA. The antigen ELISA was adapted from previously described procedures (15) with modifications. Briefly, plates were coated with the guinea pig hyperimmune antiserum to HS66 VLPs diluted 1:5,000 in coating buffer and incubated at 4°C overnight. Blocking was performed as described for the antibody ELISA. Rectal swab fluids and serum were diluted 1:10, and IC were diluted 1:40 before addition to duplicate wells. The plates were incubated for 3 h at 37°C. Rectal swab fluids and IC samples from mock-inoculated pigs and preinoculation rectal swab samples from HuNoV-inoculated pigs were used as negative controls along with wells coated with preinoculation guinea pig serum. The original HS66 sample was used as a positive control. Rabbit anti-MD145 VLPs (1:3,000) followed by goat anti-rabbit IgG conjugated to HRP (1:2,000) were added, and the plates were incubated for 1 h at 37°C. Plates were washed four times between each step with PBS containing 0.5% Tween 20 (except after the rectal swab fluid/IC, which were washed six times). The assay was developed with tetramethylbenzidine and incubated for 15 to 20 min at Rt and stopped with HCl (0.1 M). Positive samples were those with an absorbance equal to or greater than the cutoff which was determined as the mean of the negative control wells plus three times the standard deviation.

Fluorescent microscopy. Segments of duodenum, jejunum, and ileum from inoculated pigs euthanized in the acute diarrhea phase ($n = 31$) or samples from age-matched, mock-inoculated pigs ($n = 8$) were collected. Indirect immunofluorescence was performed on paraffin-embedded sectioned intestinal tissues or on whole-mount samples.

(i) Indirect immunofluorescence using paraffin-embedded intestinal tissues. The procedure was modified from the protocol described by Shoup et al. (43). Intestinal tissues were fixed in 10% neutral formalin for 10 to 18 h, dehydrated in a graded ethanol series, and embedded in paraffin. Five-micrometer sections were cut and collected on positively charged glass slides (Fischer Scientific, PA). Slides were kept at 60°C for 20 min, deparaffinized in xylene twice for 5 min, and rehydrated through the graded ethanol series. To unmask the antigens, proteinase K (DAKO, Carpinteria, CA) treatment was applied to the slides for 3 min, and then the slides were washed in PBS and blocked with 1% normal goat serum for 20 min at Rt. A primary monoclonal antibody (MAb) NS14 (1:500) was incubated overnight at Rt. This MAb (21), kindly provided by M. K. Estes (Baylor College of Medicine, TX), has been mapped to an epitope in the C terminus of the P1 domain of the capsid protein of all GII NoVs tested (33). The controls included HuNoV-infected pigs and mock-inoculated controls tested with a MAb to the spike protein of an unrelated virus (transmissible gastroenteritis virus 25C9) (43) and age-matched, mock-inoculated pigs tested with MAb NS14. Samples were washed twice with PBS and the secondary antibody, goat anti-mouse $F(ab')_2$ IgG labeled with AlexaFluor488, which produces green immunofluorescence (Invitrogen; A11075), was applied at a 1:400 dilution for 1 h at Rt. Cell nuclei were counterstained with propidium iodide, which produces a red color (Invitrogen; P1304MP), following the manufacturer's instructions.

(ii) Indirect immunofluorescence on whole intestinal tissue mounts. The intestinal tissues were fixed with 4% paraformaldehyde–0.2% glutaraldehyde in 0.1 M potassium phosphate buffer (PPB), pH 7.4, for 2 h at Rt, washed four times with PPB, and quenched with PPB containing 50 mM glycine for 1 h at Rt or kept overnight at 4°C. After permeabilization with 0.1% Triton X-100 in PBS for 1 h at Rt, tissues were washed with PBS, blocked with PBS containing 2% bovine serum albumin–5% normal goat serum for 30 min at Rt, and incubated with MAb NS14 (1:500) (21, 33) overnight at 4°C in the incubation buffer (10 mM potassium phosphate buffer [pH 7.4] containing 150 mM NaCl, 10 mM sodium azide, and 0.2% bovine serum albumin). After six washes with PBS, incubation with a 1:600 dilution of the secondary antibody, goat anti-mouse IgG (Invitrogen; A11075) labeled with AlexaFluor488, which produces a green color, in incubation buffer was performed overnight at 4°C. Samples were counterstained with the nuclear stain SYTOX orange (Invitrogen; S11368), giving a red color, and the actin stain AlexaFluor633-labeled phalloidin (Invitrogen; A222884), producing a blue color. In double-labeling experiments, we used the MAb NS14 for the viral capsid and a guinea pig antiserum to the viral N-terminal protein (r"2A"; NIH no. 60,000) from the NoV GII/4 MD145 strain (kindly provided by K. Green, NIH) (1:500) as primary antibodies and the prehyperimmunization serum of the same guinea pig (NIH no. 59,478) as control. We also used a 1:600 dilution of the AlexaFluor488-labeled goat anti-mouse IgG (Invitrogen; A11075), and the AlexaFluor576/603-labeled goat anti-guinea pig $F(ab')_2$ IgG (Invitrogen; A11017), providing a red color, as secondary antibodies. Cell nuclei were counterstained with TO-PRO-3 iodide (642/661) dye (Invitrogen; A22284), which produces a blue color, following the manufacturer's instructions. Samples were examined using a Leica model TCS-SP laser scanning confocal microscope (Leica, Wetzlar, Germany).

Histologic examination. In addition to the intestinal tissues, pieces of lungs, kidneys, livers, spleens, and mesenteric lymph nodes were collected from seven virus-inoculated and two control pigs. Tissues were fixed in 10% neutral formalin for five days, dehydrated in a graded ethanol series, embedded in paraffin, cut in 5-micrometer sections, and collected on glass slides (51). Deparaffinization was performed by placing the slides in xylene twice for 5 min with rehydration through the graded ethanol series before being stained with Mayer's hematoxylin and eosin and examined microscopically.

Detection of apoptosis. Apoptosis was examined in the epithelial cells of small intestinal tissue sections (duodenum) of five HuNoV-inoculated pigs (two pigs from group A, one pig from group B, and two pigs from group C, none of which were treated with dexamethasone) and five mock-inoculated control pigs by terminal deoxynucleotidyltransferase (TdT) for the TdT-mediated dUTP nick end labeling (TUNEL) reaction. This technique detects endonucleolysis by incorporating labeled nucleotides into DNA strand breaks. An in situ cell death detection kit (Roche) was used for paraffin-embedded tissues as directed by the manufacturer and was developed with 3-amino-9-ethylcarbazole substrate (Vector Labs). Quantification was performed by counting the total number of apoptotic cells on one field at a total magnification of ×20. Positive (DNase I-treated) and negative (no TUNEL) slides were included each time the test was performed as indicated by the manufacturer.

Transmission electron microscopy. Segments of the duodenum, jejunum, and ileum from inoculated pigs euthanized in the acute phase ($n = 10$) and confirmed positive for HuNoV by RT-PCR or mock-inoculated, age-matched control pigs ($n = 3$) were collected and transferred immediately to the fixative (3% glutaraldehyde–1% paraformaldehyde in 0.1 M PPB, pH 7.4) and then trimmed to 0.2-cm^2 pieces, and fixation was continued for 2 to 3 h at Rt. After washing once with PPB and three times with distilled water, tissue samples were postfixed with 1% osmium tetroxide and 1% uranyl acetate in distilled water for 1 h at Rt, washed three times with distilled water, dehydrated in a graded ethanol-acetone series, and embedded in Spurr's resin (Electron Microscopy Sciences, Hartfield, Pa.). For each pig, 10 thin sections (80 nm) from three blocks at three different levels were cut using diamond knives, collected on 200-nm mesh copper grids, and stained with 2% aqueous uranyl acetate and Raynold's lead citrate stain. Samples were viewed using a Hitachi H-7500 (Hitachi, Tokyo, Japan) transmission electron microscope. Transmission electron microscopy was also used for testing the reactivity of convalescent pig serum to HS66 VLPs using IEM as described previously (15).

Statistical analysis. The Fischer's exact test was used to evaluate the proportion of pigs with RT-PCR or antigen ELISA-positive IC or positive immunofluorescence of the intestinal tissues at euthanasia (early, PID 2 to 3; or late, PID 4 to 5). This test was also used to determine the proportion of pigs that seroconverted in each inoculum group and the proportion of pigs with dexamethasone treatment that showed diarrhea or had fecal virus shedding. The Kruskal-

TABLE 1. Detection of HuNoV GII/4 HS66 virus by RT-PCR and antigen ELISA of IC and indirect immunofluorescence of small intestinal tissues of HuNoV-inoculated and mock-inoculated Gn pigs euthanized in the acute phase of disease[a]

Group	Inoculum[b]	No. of pigs	Euthanasia (PID)	Diarrhea at euthanasia[c] (%)	IC RT-PCR (%)	IC Ag ELISA (%)	IF gut tissues[d] (%)
A	P0	16	2–3	12/16 (75)	9/16 (56)	6/16 (38)	8/14 (57)
		10	4–5	8/10 (80)	2/10 (20)	2/10 (20)	4/7 (57)
B	P1	5	2–3	4/5 (80)	2/5 (40)	1/5 (20)	2/3 (67)
		6	4–5	5/6 (83)	1/6 (17)	0/6 (0)	2/3 (67)
C	P2	6	2–3	3/6 (50)	3/6 (50)	0/6 (0)	2/4 (50)
Total		43		32/43 (74)	17/43 (40)	9/43 (21)	18/31 (58)
Control[e]	Mock	8	2–5	0/8	0/8	0/8	0/8

[a] Acute phase, PID 2 to 3 and PID 4 to 5.
[b] Oral inoculation using 5 ml of 1:10 stool filtrate or serial passaged intestinal IC. P0, original sample; P1, IC RT-PCR positive from a pig inoculated with P0; P2, IC RT-PCR positive from a pig inoculated with P1.
[c] Number of positive pigs/total number of pigs tested.
[d] Detected by indirect IF.
[e] Mock inoculation with 5 ml MEM.

Wallis test (nonparametric) was used to compare the onset and duration of diarrhea and shedding in each inoculum group. As no increase in severity or duration of diarrhea or fecal viral shedding was observed, the dexamethasone-treated pigs were analyzed together with the untreated pigs. Correlations between viral shedding, diarrhea, and seroconversion were analyzed by use of Pearson's correlation coefficient. Statistical significance was assessed at a P value of <0.05. The data were analyzed using the Statistical Analysis Systems (SAS Institute Inc., Cary, NC).

RESULTS

Characterization of the original HS66 sample (P0) and P1 and P2 inocula. The original HS66 (P0) and the P1 and P2 inocula were screened for NoV particles by IEM using the guinea pig antiserum to NoV GII/4 VLPs. Viral particles with NoV size and morphology were observed in the original sample and one of the P1 samples but not in the P2 sample, likely due to low viral concentration. No other viruses were observed.

The actual processed inocula were quantified by real-time RT-PCR as having approximately the following GE/ml: P0, 5×10^5; P1, 1×10^2; and P2, 8. However, at low copy numbers quantification is less reliable, so these only represent GE estimates. Sequencing data from the product of Mon primers 431/433 (211 bp) targeting the RdRp and Mon 381/383 (320 bp) targeting the 5′ end of the capsid in the original sample and after each passage confirmed the product specificities but did not reveal any mutations in these regions. The amplification and sequencing of the hypervariable region in ORF2 has been elusive, possibly due to mutations in the primer targeting sequence or low viral RNA concentration. The sequencing of the whole ORF2 of the virus in the P1 and P2 inocula has also been unsuccessful, possibly because amplification of larger products is more difficult to obtain with the low amounts of virus present in the passaged samples.

Presence of diarrhea, fecal viral shedding, viremia, and seroconversion. The data on diarrhea and viral shedding (onset and duration), seroconversion, and detection of infected cells in the intestinal tissues by IF are summarized in Tables 1 and 2. Diarrhea was observed in 74% (48/65) of the inoculated pigs, occurring from PID 1 (average onset, PID 2) and persisting up to PID 5 (average, PID 2) (pigs included in Tables 1 and 2). Most pigs with clinical manifestations showed mild diarrhea (score, 2), with only a few showing more severe diarrhea. Forty-four percent (29/65) of the inoculated pigs shed virus in feces as detected by RT-PCR from PID 1 to a maximum of 4 days (average duration of 3 days, although some pigs shed for 1 day only). Shedding was detectable for longer in some cases (up to 8 days) (data not shown) by amplicon hybridization,

TABLE 2. Diarrhea and fecal virus shedding detected by RT-PCR and seroconversion detected by antibody ELISA in Gn pigs inoculated with the HuNoV GII/4 HS66 strain or mock-inoculated Gn pigs maintained through PID 21

Group	Inoculum[a]	No. of pigs orally inoculated	Diarrhea (%)[b]	Mean onset of diarrhea (PID)	Mean duration of diarrhea (days)	Fecal virus shedding (%)	Mean onset of fecal virus shedding (PID)	Mean duration of fecal virus shedding (days)	Seroconversion[c] (%)
A	P0	10 (+1 i.v.)[d]	7/11 (64)	2	2	8/11(73)	1	3	7/11 (64)
B	P1	6 (+1 i.v.)	6/7 (86)	2	3	2/7 (29)	1	2	4/7 (57)
C	P2	4	3/4 (75)	2	1	2/4 (50)	2	2	2/4 (50)
Total		22	16/22 (73)	2	2	12/22 (55)	1.3	2.3	13/22 (59)
Control[e]	Mock	6	0/6	N/A[f]	N/A	0/6	N/A	N/A	0/6

[a] Oral inoculation using 5 ml of 1:10 human stool filtrate (HS66) or serial passaged IC. P0, original sample; P1, IC RT-PCR positive from a pig inoculated with P0; P2, IC RT-PCR positive from a pig inoculated with P1.
[b] Number of positive pigs/total number of pigs tested.
[c] Detected by antibody ELISA (IgG).
[d] One pig was inoculated by the intravenous (i.v.) route.
[e] Mock inoculation with 5 ml MEM.
[f] N/A, not applicable.

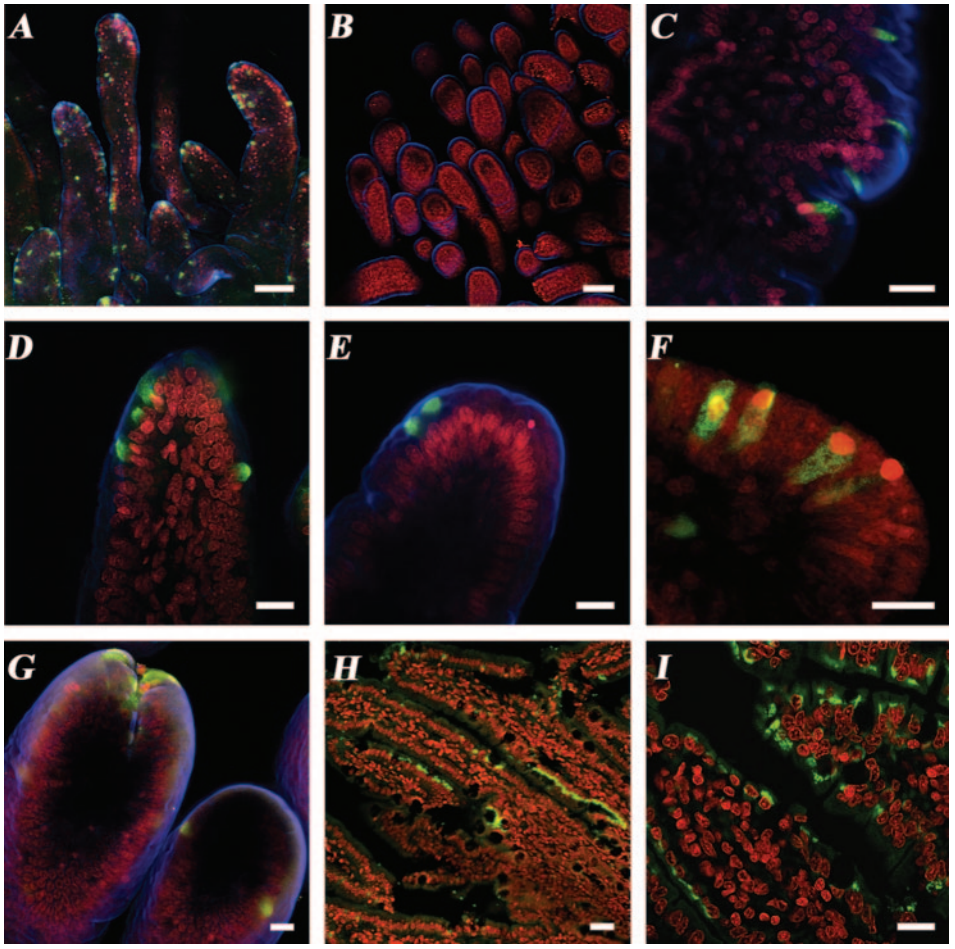

FIG. 1. Confocal microscopy showing indirect immunofluorescent localization of the HuNoV capsid protein in small intestinal tissues from virus-inoculated Gn pigs. (A to G) IF on whole-mount tissues. (H to I) IF on tissue paraffin sections. Primary antibody NS14 MAb was used to detect the capsid protein of HuNoV GII. Secondary antibodies: goat anti-mouse IgG Alexa488 (green) (nuclear counterstain [A to G] SYTOX orange [red] or propidium iodide [H to I] [red]) and actin stained with phallotoxin Alexa633 (blue). (A) Jejunum of a P2-inoculated Gn pig at PID 3 showing scattered IF-positive cells on the villi tips or sides. (B) Jejunum of a mock-inoculated pig with no IF-positive cells evident. (C) Jejunum of a P1-inoculated Gn pig at PID 3, showing individually infected enterocytes on the side of a villus. (D) Tip of a villus in the duodenum of a P1-inoculated Gn pig at PID 3 with several contiguous infected cells. (E) Tip of a villus on the jejunum of a P1-inoculated Gn pig at PID 3 with positive signal in the apical portion of the enterocyte cytoplasm. (F) Enterocytes from the duodenum of a P0-inoculated Gn pig at PID 3, showing nuclear displacement and positive signal throughout the cytoplasm of individual cells. (G) Tip of a villus in the duodenum of a P0-inoculated pig at PID 2 showing contiguous infected cells. (H) Paraffin section of the duodenum of a P0-inoculated Gn pig at PID 4 showing contiguous infected enterocytes on the sides of the villi and some individual enterocytes on the tips. (I) Higher magnification, most enterocytes showed perinuclear IF. Bars: A and B, 100 μm; C to H, 20 μm.

which is more sensitive than gel electrophoresis (49). According to real-time RT-PCR, the fecal viral shedding after each passage was lower than that of the original inoculum. This was reflected in the P0, P1, and P2 GE/ml as noted earlier. Twenty-one percent of the IC from virus-inoculated pigs euthanized in the acute phase (PID 2 to 3 or 4 to 5; Table 1) were positive for viral antigen by Ag ELISA and 39% (17/43) for viral RNA by RT-PCR, respectively. In P0-inoculated pigs, more IC were positive by RT-PCR and AgELISA when pigs were tested early (PID 2 to 3) ($P = 0.09$). There were significant differences for the duration of virus shedding between inoculum passages ($P = 0.004$), with P0-inoculated pigs having significantly longer viral shedding than P1- and P2-inoculated pigs (Table 2). Viral shedding correlated moderately with seroconversion ($r = 0.4$; $P = 0.02$) and with diarrhea ($r = 0.3$; $P = 0.003$), but diarrhea was more highly correlated with seroconversion ($r = 0.7$; $P = <0.001$).

From the two pigs inoculated by the intravenous route, only the one inoculated with P0 shed virus in feces, whereas the pig inoculated with P1 did not, although both had mild signs of diarrhea. The Gn pigs treated with dexamethasone at the given dose and period of time did not differ statistically in diarrhea or virus shedding compared to HuNoV-inoculated, non-dexamethasone-treated pigs. The mock-inoculated Gn pigs treated with the same dexamethasone regimen did not develop diarrhea. Five of eight P0-inoculated pigs tested had HuNoV RNA detected by RT-PCR in serum on PID 1 ($n = 3$) or 2 ($n = 2$); sera from the other three P0-inoculated and two mock-inoculated controls were negative for viral RNA during the 10 days tested (data not shown). Four of five viremia-positive pigs were

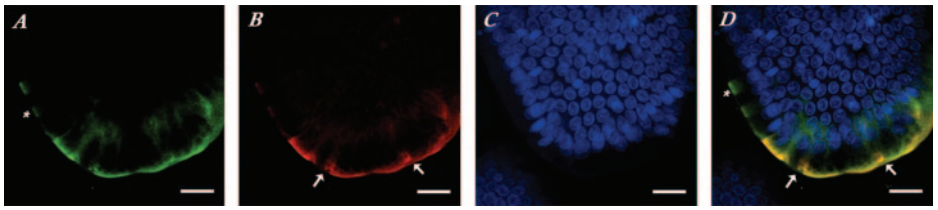

FIG. 2. Confocal microscopy of immunofluorescent colocalization of viral capsid and N-terminal protein antigens in whole-mount small intestinal tissue. (A) Anti-capsid NS14 MAb with the secondary goat anti-mouse IgG antibody conjugated to Alexa488 (green). (B) Antiviral N-terminal protein guinea pig serum with the secondary goat anti-guinea pig IgG labeled with AlexaFluor576/603 (red). (C) Cell nuclei were counterstained with TO-PRO-3 iodide (642/661) dye (blue). (D) Merged image where the yellow color indicates colocalization of viral capsid and N-terminal protein antigens. Asterisks indicate cells where only the capsid protein was detected, and arrows indicate apical globular-like structures detected with the anti-N-terminal protein serum. Bars, 20 μm.

also confirmed by antigen ELISA. Seroconversion occurred in 59% of the inoculated pigs (Table 2), independent of the HS66 pig passage number, but with low to moderate geometric mean serum IgG antibody titers (titer range, 20 to 200; data not shown). None of the mock-inoculated control pigs developed antibodies to HuNoV. We confirmed the seroconversion results using the immunostaining assay for the HS66 capsid recombinant baculovirus-infected Sf9 cells. Also, convalescent pig serum (diluted 1:50) reacted with HS66 VLPs (2 μg), as noted by its extensive coating and occasional clumping of the particles as observed by IEM.

Identification of infected cells by IF. Confocal fluorescent microscopy was used to confirm HuNoV infection of the Gn pig small intestinal tissues and to characterize the infection at the cellular level. We performed IF localization using paraffin sections and whole-mount small intestinal tissue samples. The first method allows the visualization of deeper portions of the small intestine and permits testing of archived samples in paraffin blocks, whereas the whole-mount tissue method may be more sensitive because there is no masking of the antigens by embedding but it requires fresh tissues.

Immunofluorescence of whole-mount small intestinal segments from virus-inoculated pigs showed that the distribution of positively (green) stained enterocytes was patchy and in discrete areas in the villi of the duodenum and jejunum (Fig. 1A, C, D, E, and G), and only a few stained cells were found in the ileum (data not shown). Similar results were obtained with tissues in paraffin sections (panels H and I). No cells were stained in the intestinal tissue samples from the mock-inoculated pig (Fig. 1B). In the infected regions, individual epithelial cells or a few clustered cells exhibited viral antigen in their cytoplasm in a punctate pattern (Fig. 1C and F). Positive enterocytes were located predominantly at various sites, at the tips (Fig. 1D, E, and G) or sides of each villus (Fig. 1A and C). Viral capsid antigen was detected at different locations within the cell cytoplasm in both whole-mount tissues and paraffin sections: in some cases the signal was perinuclear (Fig. 1D, E, and I), apical (Fig. 1E), or diffuse (Fig. 1C, D, F, and H) but was not observed in the nucleus (in Fig. 1D, the signal was perinuclear, as confirmed by sectional images; data not shown). Positive IF for the viral capsid antigen in paraffin sections was observed in deep areas of the duodenum in only a few pigs (data not shown). It is unclear whether the antigen was located in Brunner glands or crypts. More pigs need to be analyzed to confirm if replication is occurring there or if binding and internalization occurred because the putative NoV receptors (HBGA) are expressed in this location.

Small intestinal tissue samples of pigs positive by RT-PCR from 12 of 21 (57%) pigs also tested positive by IF in the group inoculated with P0 (Table 1), as well as four of six (66%) pigs from the P1-inoculated group and two of four (50%) pigs inoculated with P2. We could not detect the virus by IF in the small intestines of some pigs that were positive by RT-PCR although IF permits evaluation of only a few areas and cells of the small intestine of each pig.

To evaluate if the HuNoV replicated in the small intestinal cells, we used an antibody to the nonstructural N-terminal viral protein. We detected positive signals in the HuNoV-inoculated pigs (Fig. 2B and D) although the distribution of infected small intestinal cells detected by this antibody was limited (data not shown). Fluorescent coimmunolocalization of whole-mount intestinal tissues also demonstrated that the N-terminal protein antigen was detected in enterocytes that also exhibited the presence of the capsid protein antigen (Fig. 2A, B, and D). In some cells that showed positive signal for the capsid antigen, the N-terminal antigen was not detected (see asterisks in Fig. 2A and D). In addition, although the capsid antigen was detected at various locations throughout the cell cytoplasm, the N-terminal antigen localization was only apical and in some cases formed globular-like structures (Fig. 2B and D).

Histopathologic examination. Intestinal segments of HuNoV ($n = 7$) and mock-inoculated ($n = 2$) pigs euthanized from PID 2 to 5 were examined for the presence of macroscopic and microscopic lesions. Only 1 of 7 HuNoV P0-inoculated pigs euthanized at PID 4 had mild pathological changes. These included moderate multifocal villous atrophy (30 to 40% of the villi), villus enterocytes with low columnar morphology, and mild foamy cytoplasm and subtle edema of the lamina propria in the duodenum. No pathological changes were seen in the jejunum and ileum.

Apoptosis in the small intestinal tissues of HuNoV-inoculated pigs. Because few infected pigs showed macroscopic and microscopic small intestinal lesions, we used the TUNEL reaction to evaluate whether infected enterocytes were dying by apoptosis instead of lysis and if apoptosis was occurring at a higher rate in infected pigs than in controls. Apoptotic cells were counted at a ×20 magnification in 10 villi from a single section for each pig. All of the HuNoV-inoculated pigs showed increased numbers of apoptotic cells per microscopic field (20 to 70 cells) compared to those for mock-inoculated control pigs

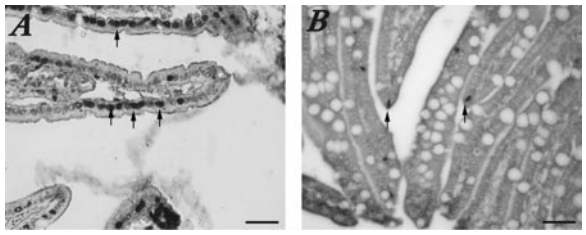

FIG. 3. TUNEL reaction to detect apoptotic cells in small intestinal tissues of HuNoV-inoculated and mock-inoculated pigs. (A) More cells with dark-staining apoptotic nuclei (arrows) were observed in HuNoV P0-inoculated Gn pig duodenum. (B) TUNEL results showing fewer apoptotic cells and more goblet cells (not evident in the infected pig) in a mock-inoculated control Gn pig. Bars, 50 μm.

(3 to 7 cells) (Fig. 3). No pigs treated with dexamethasone were analyzed.

Detection of calicivirus-like particles by TEM in small intestinal tissues. The ultrastructural morphology and the presence of HuNoV-like particles in the small intestines from HuNoV-inoculated ($n = 10$) and mock-inoculated ($n = 3$) Gn pigs were analyzed by using TEM (Fig. 4A to E). Whereas most of the small intestinal tissues from HuNoV-inoculated Gn pigs did not show abnormalities, we noted enterocytes with cytoplasmic vesicles of 400 nm to 1.5 μm in diameter (Fig. 4A) containing calicivirus-like particles of 25 to 40 nm in diameter (Fig. 4C and D) in the small intestinal TEM sections of three pigs at PID 3 (two pigs from group A and one from group C). These particles were seen within or next to membrane structures in the cytoplasm (Fig. 4C, D, and E). No viral particles were found in the nucleus. Some cells also had changes in their intracellular organization, with nuclear displacement and decrease of organelle numbers (Fig. 4A and C). Such vesicles and calicivirus-like particles were not present in tissue samples from the mock-inoculated pigs (Fig. 4B).

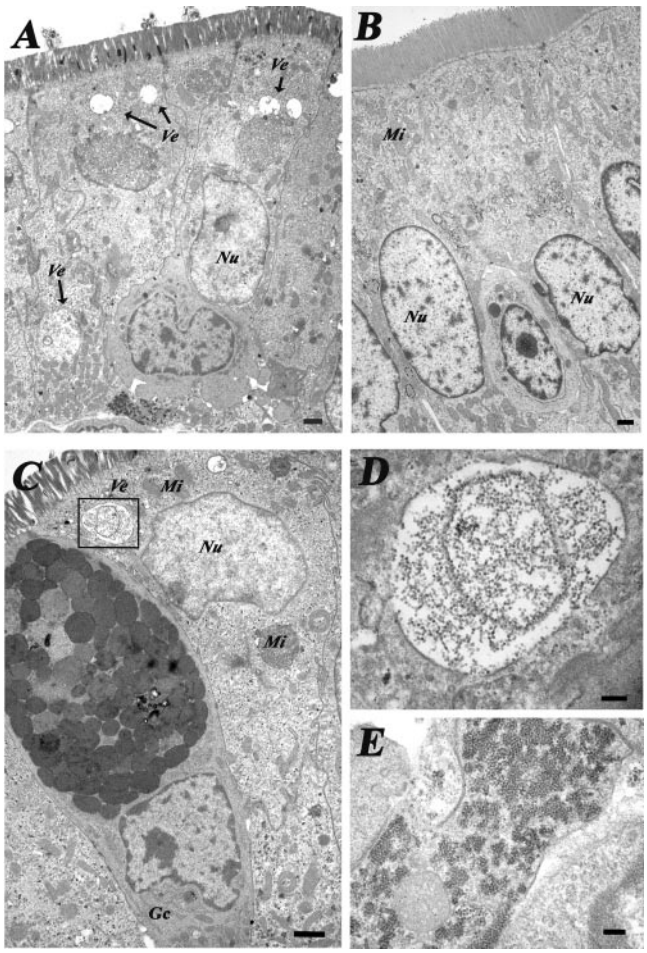

FIG. 4. Transmission electron microscopy of (A) the jejunum of a HuNoV GII/4 P0-inoculated Gn pig at PID 3 with the nucleus displaced opically. The arrows indicate vesicles (*Ve*) not seen in the control Gn pig. (B) Cells showed changes in their intracellular organization, with cellular organelles decreased in number. (B) Jejunum of an age-matched, mock-inoculated control pig. (C to E) Duodenum of a P0-inoculated Gn pig at PID 3. (C) The overall intracellular morphology of the enterocyte is disrupted, with vesicles in the cytoplasm containing calicivirus-like particles (box) and nuclear (*Nu*) displacement; mitochondria (*Mi*) are indicated. A goblet cell (*Gc*) can be observed. (D) Detail of the membrane vesicle, from the box in panel C, containing calicivirus-like particles. (E) Aggregates of calicivirus-like particles in the cytoplasm of another cell. Bars: A to C, 1 μm; D, 200 nm; E, 225 nm.

DISCUSSION

Mild diarrhea was observed in most, but not all, HuNoV-inoculated pigs from the same litter, suggesting that genetic variability among individuals may play a role in pigs as it does in humans (39). The incubation period was 24 to 48 h, and the diarrhea was mild and of short duration (1 to 3 days), similar to what has been described in human volunteers (12, 54). Thus, the HuNoV in Gn pigs caused an acute and self-limiting disease as it does in its original host. Detection of fecal virus shedding was short (1 to 4 days by RT-PCR, but longer by amplicon hybridization, through PID 8). Longer asymptomatic shedding has been described in some normal humans, where 28% of infected individuals shed virus for up to 3 weeks after the onset of disease (38). Similar results were observed in a trial involving pigtail macaques inoculated with Toronto virus (HuNoV GII/3) (45). The fact that the amount of virus after each pig passage was lower than that contained in the original inoculum does not necessarily mean that adaptation to the pig has not occurred. The NoVs, like other RNA viruses, probably exist as quasispecies whereby one clone is predominant under the existing conditions because it is better fit, but when conditions change (for example in an alternative host), other clones may be more fit to the new conditions and a different clone will dominate. However, this selection may need multiple pig passages to adequately amplify the new clone (17). Therefore, it may take several passages before we detect an increase in viral shedding. The lower infection rates in the P1- and P2-inoculated groups may indeed reflect the lower viral doses they received. Nevertheless, similar to human NoV infections, even low doses appear to be infectious, as confirmed by detection of viral infected intestinal cells in pigs at each passage level, albeit fewer pigs became infected when using the P2 inoculum. The possibility that we were detecting the pass-through inoculum in the small intestines cannot be excluded for day 1, but detection beyond this time is improbable. In addition, we couldn't detect viral antigen, viral RNA, or antibodies to HuNoV in two pigs

inoculated orally with inactivated virus (data not shown). This is in contrast to what was described in a study where common marmosets and tamarins orally inoculated with Norwalk virus shed virus for 3 to 4 days but no clinical signs or antibody responses were detected so it remained unclear whether viral replication occurred (39). The viral dose was higher for the P0-inoculated pigs than for the P1- and the P2-inoculated pigs, and this may explain the lower rate of infection in the later groups. In our study, most of the pigs had diarrhea and half of them seroconverted. Moreover viral antigen was also observed in the cytoplasm of the intestinal epithelial cells of these pigs. In addition, we demonstrated that the viral N-terminal protein was present in the infected cells (Fig. 2B), showing that the virus was taken up by the enterocytes and translation of viral nonstructural proteins also occurred. We attempted to mimic an immunosuppressed state, with dexamethasone treatment, such as that occurring in transplanted individuals. We did not observe an increase in severity or duration of diarrhea or fecal viral shedding with the given dose during the given time frame; therefore, these animals were analyzed with the untreated pigs.

Viral RNA (5/8 pigs) and viral antigen (4/8 pigs) were detected in the serum of P0 orally inoculated pigs on PID 1 or 2, demonstrating the existence of transient viremia. Because no lesions were observed in any organs other than the small intestine, the impact of the viremia on the pathogenesis of the disease is unknown. The pigs that had virus in their serum still developed low serum IgG antibody titers to HS66, maybe because the viremia was very short-lived (less than 1 day). Similar percentages of viremia were detected in P0-, P1-, and P2-inoculated pigs in a more extensive study (Souza, Cheetham, and Saif, unpublished). Viremia has been detected for other enteric viruses such as the porcine sapoviruses (PEC/Cowden) in pigs and human rotavirus in humans, mice, and pigs without causing lesions outside the small intestines (4, 5, 14). As described for PEC/Cowden (14), we report that one pig inoculated intravenously with P0 showed viral shedding and diarrhea. However, a P1 intravenously inoculated pig did not develop infection (data not shown).

In our study, seroconversion occurred in 59% of the inoculated pigs with low to moderate antibody titers ranging from 20 to 200, independent of the inoculum passage used. This was perhaps because the duration and severity of the infection was too limited to induce a strong IgG immune response or due to the insensitivity of our ELISA. Because the antibody titers of Gn pigs were low, we used the baculovirus-expressed capsid protein immunostaining assay to further confirm seroconversion. Also, we are reporting IgG seroconversion although some pigs had more prominent serum IgA antibody responses, whereas others had more prominent serum IgG antibody responses (Souza, Cheetham, and Saif, unpublished). Because the Gn pigs are completely naive to these viral antigens, their immune responses cannot be accurately compared to those of adult humans who have likely been repeatedly exposed to NoV since early childhood (32). The antibody responses in humans may be of higher magnitude because, although long-term memory may not be as efficient in NoV infections as for other diseases and complete protection does not exist between strains from different genogroups (24), there are common epitopes within and between genogroups (33) that likely cause a stronger immune response after repeated NoV exposure. Nevertheless we have also detected specific immune responses from pigs exposed to this GII/4 strain by B-cell enzyme-linked immunospot assay and cytokine ELISA (Souza, Cheetham, and Saif, unpublished; presented at the American Society for Virology 25th Annual Meeting, University of Wisconsin—Madison, Madison, Wis., 15 to 19 July 2006). Similar findings have been reported for macaques inoculated with Toronto virus (45) and Rhesus monkeys inoculated with Norwalk virus where infection occurred in both the presence and absence of seroconversion (6). In another study where three Rhesus monkeys were inoculated with Norwalk virus, only the monkey that shed virus for 19 days seroconverted to Norwalk virus whereas the other two monkeys that shed for 1 to 2 days did not (39). Therefore, long-term shedding, a high amount of virus replication, or repeated exposures to HuNoV may be necessary to induce a strong immune response in naive animals.

In this study, ELISA, RT-PCR, and amplicon hybridization results varied from animal to animal, similarly to what has been previously described by others when inoculating monkeys with the NoV GII/3 Toronto strain (45). Therefore, all three tests were necessary to ensure viral detection. We observed both pigs that shed virus without showing signs of diarrhea and also pigs with diarrhea that were negative for viral shedding. The latter observation may be due to the viral shedding being below the detection limit or to the presence of fecal inhibitors. In some cases the effect of RT-PCR inhibitors was diminished by dilution of the RNA, but as a consequence the assay sensitivity was also decreased (49). By IEM, only a few viral particles were detected in only 1 of 15 pigs' intestinal contents tested at PID 3, indicative of very low concentrations of virus shedding ($<10^6$ viral particles/ml). Shedding of low quantities of virus has also been reported for humans and monkeys (45).

In some pigs that were positive by RT-PCR, viral antigen was not detected by IF or by TEM. This could be due to the limited intestinal areas inspected for each pig using these techniques, a lower extent of the infection, or the rapid extrusion of infected epithelial cells prior to euthanasia.

Histopathologic examination showed mild lesions in the upper intestines of only 1 of 7 pigs. We speculate that because of the mild diarrhea and detection of scattered, patchy infected cells by IF, the histopathologic lesions in pigs are subtle or absent. Moreover, if most infected cells or bystander cells die by apoptosis, cytopathic lesions in the intestinal tract may be absent. It is likely that in our experiments, the HuNoV HS66 strain did not replicate as efficiently in pigs as in the host species. We expect that adaptation by further serial passage in the pig may increase the pathogenicity for the new host.

In addition, extensive histopathologic lesions may not be apparent in the Gn pig's intestine because the HuNoV-infected enterocytes may be dying by apoptosis and not lysis. All the intestinal tissues from the HuNoV-inoculated pigs examined showed increased numbers of TUNEL-reactive cells compared to the control pig tissues. Although the TUNEL reaction may detect both apoptotic and necrotic cells, the morphology of the infected cells observed by TEM and IF (nuclear displacement, chromatin condensation, and reduced number of organelles) suggests apoptosis rather than necrosis may result from NoV replication in the enterocytes. Apoptosis has also been described for other members of the *Caliciviridae* family. Apoptosis of hepatocytes was observed in naturally infected

rabbits with rabbit hemorrhagic disease virus, causing severe pathology that usually results in death (3). Apoptosis has also been described for feline calicivirus (FCV) infection of cell cultures (2, 37, 44). Of interest, induction of apoptosis by FCV requires active viral replication (44). Clinical cases of allograft lesions from pediatric intestinal transplant patients were common to allograft rejection, but increased superficial apoptosis was characteristic of HuNoV enteritis, whereas crypt apoptosis was common to both. Apoptotic bodies were present in epithelial cells, and macrophages containing apoptotic bodies were observed in the villous lamina propria. Surprisingly, in the Gn pigs examined, the extrusion zones of the villi of both infected and uninfected pigs did not show many apoptotic cells. This may be because the villus enterocyte turnover rates in Gn pigs are slower than in conventional pigs of similar ages (30). Moreover, in mouse small intestine, shedding of enterocytes from these zones usually occurs prior to detectable cellular activation of caspase 3 or nuclear condensation (52). Data from a microarray study of mouse gene expression in intestinal epithelial cells along the crypt-villus axis supports these findings (25). No up-regulation of apoptosis-related genes was observed in the villous enterocytes, although more than a thousand genes were differentially expressed. More studies are necessary to determine the role and the mechanism of apoptosis in the pathogenesis of HuNov in Gn pigs.

We observed different patterns of viral antigen distribution within the cell (perinuclear, apical, or diffuse) that may represent different stages of the viral replication cycle. The N-terminal protein antigen was detected in the apical portion of the enterocytes, forming in some cases globular-like structures (Fig. 2B). We speculate that these may be the membranous vesicles containing calicivirus-like particles that were observed by TEM (Fig. 3A and C). As described for other positive-stranded RNA viruses that replicate in association with cellular membranes (41), these globular structures or vesicles may represent virus replication sites. The membranous vesicles containing the calicivirus-like particles may have originated from a cellular organelle, as described for other members of the *Caliciviridae* family such as FCV (13). In in vitro experiments, the nonstructural N-terminal protein encoded by the 5′ region of ORF1 for both GI (Norwalk virus) and GII (MD145 GII/4) NoVs was associated with Golgi apparatus localization, and there was a discrete time course in the disassembly of the Golgi complex into aggregates generating two patterns: one of marked discrete aggregates and the other a more diffuse distribution of the protein throughout the cytoplasm (10).

The TEM images showed cells with morphological changes and the presence of viral particles similar to what has been described for murine NoV 1 infection of macrophages in vitro (53). Contrary to what has been described for infection of epithelial cells in cats by FCV (35), which belongs to the *Vesivirus* genus, no viral particles were observed in the nucleus.

In humans, genetic factors such as polymorphisms in the *FUT1* (H), *FUT2* (Se), and *FUT3* (Le) genes that code for glycosyltransferases responsible for producing carbohydrate chains have been associated with susceptibility to NoV GI and II (23, 26, 27). At present we are evaluating reagents and assays to test for HBGA in pigs to ascertain if the same or similar genetic factors influence NoV infection of Gn pigs.

Similar to the human population, pigs infected with HuNoVs showed various degrees of resistance, susceptibility, presence or absence of seroconversion, and severity and duration of clinical signs and viral shedding. For these reasons, the Gn pig model may be useful to study the pathogenesis of HuNoV infections. Because less than 100% of the pigs became infected, further serial pig passage of virus and other variables may need to be assessed to increase infection and diarrhea rates in this model (pig HBGA types, etc.). Nevertheless, serial passage of the virus in pigs (three passages), with virus shed at each passage, and detection of HuNoV-infected cells by IF suggests that the HuNoV from GII/4 is at least partially adapting to replication in the Gn pig host and that further adaptation may increase its pathogenicity for the pig.

ACKNOWLEDGMENTS

We thank Trang Van Nguyen and Marli Azevedo for their suggestions on statistical analysis and Veronica Costantini for technical help. We also thank J. Hughes, who kindly provided the original NoV GII/4 human fecal sample; M. Estes, who kindly provided the NS14 MAb; K. Green, who kindly provided MD145 VLPs and antiserum to MD145 VLPs and antiserum to MD145 N-terminal protein; and J. Xiang for confirming some preliminary RT-PCR results. J. Hanson and R. McCormick provided animal care. We thank Sean Smith, Scott Fox, and Jeff Hayes at the Animal Disease Diagnostic Laboratory, Ohio Department of Agriculture, Reynoldsburg, Ohio, for providing assistance with the IHC technique. We also thank Andrea Kaszas and David Fulton at the Molecular and Cellular Imaging Center who provided technical assistance with the confocal and electron microscope and D. J. Jackwood and K. W. Theil for reviewing the manuscript.

Salaries and research support were provided by state and federal funds appropriated to the Ohio Agricultural Research and Development Center, The Ohio State University. This work was funded by National Institute of Allergies and Infectious Diseases, National Institutes of Health, grant no. R0I AI49742.

REFERENCES

1. **Agus, S. G., R. Dolin, R. G. Wyatt, A. J. Tousimis, and R. S. Northrup.** 1973. Acute infectious nonbacterial gastroenteritis: intestinal histopathology. Histologic and enzymatic alterations during illness produced by the Norwalk agent in man. Ann. Intern. Med. **79:**18–25.
2. **Al-Molawi, N., V. A. Beardmore, M. J. Carter, G. E. Kass, and L. O. Roberts.** 2003. Caspase-mediated cleavage of the feline calicivirus capsid protein. J. Gen. Virol. **84:**1237–1244.
3. **Alonso, C., J. M. Oviedo, J. M. Martin-Alonso, E. Diaz, J. A. Boga, and F. Parra.** 1998. Programmed cell death in the pathogenesis of rabbit hemorrhagic disease. Arch. Virol. **143:**321–332.
4. **Azevedo, M. S., L. Yuan, K. I. Jeong, A. Gonzalez, T. V. Nguyen, S. Pouly, M. Gochnauer, W. Zhang, A. Azevedo, and L. J. Saif.** 2005. Viremia and nasal and rectal shedding of rotavirus in gnotobiotic pigs inoculated with Wa human rotavirus. J. Virol. **79:**5428–5436.
5. **Blutt, S. E., C. D. Kirkwood, V. Parreno, K. L. Warfield, M. Ciarlet, M. K. Estes, K. Bok, R. F. Bishop, and M. E. Conner.** 2003. Rotavirus antigenaemia and viraemia: a common event? Lancet **362:**1445–1449.
6. **Cubitt, W. D.** 1985. Human caliciviruses characterization and epidemiology. Ph.D. thesis. London University, London, United Kingdom.
7. **Dolin, R., N. R. Blacklow, H. DuPont, R. F. Buscho, R. G. Wyatt, J. A. Kasel, R. Hornick, and R. M. Chanock.** 1972. Biological properties of Norwalk agent of acute infectious nonbacterial gastroenteritis. Proc. Soc. Exp. Biol. Med. **140:**578–583.
8. **Dolin, R., A. G. Levy, R. G. Wyatt, T. S. Thornhill, and J. D. Gardner.** 1975. Viral gastroenteritis induced by the Hawaii agent. Jejunal histopathology and serologic response. Am. J. Med. **59:**761–768.
9. **Estes, M. K., R. L. Atmar, and M. E. Hardy.** 1997. Norwalk and related diarrhea viruses, p. 1073–1095. *In* D. D. Richman, R. J. Whitley, and F. G. Hayden (ed.), Clinical virology. Churchill Livingstone, New York, N.Y.
10. **Fernandez-Vega, V., S. V. Sosnovtsev, G. Belliot, A. D. King, T. Mitra, A. Gorbalenya, and K. Y. Green.** 2004. Norwalk virus N-terminal nonstructural protein is associated with disassembly of the Golgi complex in transfected cells. J. Virol. **78:**4827–4837.
11. **Gallimore, C. I., D. Cubitt, N. du Plessis, and J. J. Gray.** 2004. Asymptomatic and symptomatic excretion of noroviruses during a hospital outbreak of gastroenteritis. J. Clin. Microbiol. **42:**2271–2274.
12. **Graham, D. Y., X. Jiang, T. Tanaka, A. R. Opekun, H. P. Madore, and M. K.**

Estes. 1994. Norwalk virus infection of volunteers: new insights based on improved assays. J. Infect. Dis. **170:**34–43.
13. **Green, K. Y., A. Mory, M. H. Fogg, A. Weisberg, G. Belliot, M. Wagner, T. Mitra, E. Ehrenfeld, C. E. Cameron, and S. V. Sosnovtsev.** 2002. Isolation of enzymatically active replication complexes from feline calicivirus-infected cells. J. Virol. **76:**8582–8595.
14. **Guo, M., J. Hayes, K. O. Cho, A. V. Parwani, L. M. Lucas, and L. J. Saif.** 2001. Comparative pathogenesis of tissue culture-adapted and wild-type Cowden porcine enteric calicivirus (PEC) in gnotobiotic pigs and induction of diarrhea by intravenous inoculation of wild-type PEC. J. Virol. **75:**9239–9251.
15. **Guo, M., Y. Qian, K. O. Chang, and L. J. Saif.** 2001. Expression and self-assembly in baculovirus of porcine enteric calicivirus capsids into virus-like particles and their use in an enzyme-linked immunosorbent assay for antibody detection in swine. J. Clin. Microbiol. **39:**1487–1493.
16. **Han, M. G., Q. Wang, J. R. Smiley, K. O. Chang, and L. J. Saif.** 2005. Self-assembly of the recombinant capsid protein of a bovine norovirus (BoNV) into virus-like particles and evaluation of cross-reactivity of BoNV with human noroviruses. J. Clin. Microbiol. **43:**778–785.
17. **Holland, J. J., J. C. De La Torre, and D. A. Steinhauer.** 1992. RNA virus populations as quasispecies. Curr. Top. Microbiol. Immunol. **176:**1–20.
18. **Jiang, X., P. W. Huang, W. M. Zhong, T. Farkas, D. W. Cubitt, and D. O. Matson.** 1999. Design and evaluation of a primer pair that detects both Norwalk- and Sapporo-like caliciviruses by RT-PCR. J. Virol. Methods **83:**145–154.
19. **Kaufman, S. S., N. K. Chatterjee, M. E. Fuschino, M. S. Magid, R. E. Gordon, D. L. Morse, B. C. Herold, N. S. LeLeiko, A. Tschernia, S. S. Florman, G. E. Gondolesi, and T. M. Fishbein.** 2003. Calicivirus enteritis in an intestinal transplant recipient. Am. J. Transplant. **3:**764–768.
20. **Kaufman, S. S., N. K. Chatterjee, M. E. Fuschino, D. L. Morse, R. A. Morotti, M. S. Magid, G. E. Gondolesi, S. S. Florman, and T. M. Fishbein.** 2005. Characteristics of human calicivirus enteritis in intestinal transplant recipients. J. Pediatr. Gastroenterol. Nutr. **40:**328–333.
21. **Kitamoto, N., T. Tanaka, K. Natori, N. Takeda, S. Nakata, X. Jiang, and M. K. Estes.** 2002. Cross-reactivity among several recombinant calicivirus virus-like particles (VLPs) with monoclonal antibodies obtained from mice immunized orally with one type of VLP. J. Clin. Microbiol. **40:**2459–2465.
22. **Koopmans, M., J. Vinje, M. de Wit, I. Leenen, W. van der Poel, and Y. van Duynhoven.** 2000. Molecular epidemiology of human enteric caliciviruses in The Netherlands. J. Infect. Dis. **181**(Suppl. 2)**:**S262–S269.
23. **Lindesmith, L., C. Moe, S. Marionneau, N. Ruvoen, X. Jiang, L. Lindblad, P. Stewart, J. LePendu, and R. Baric.** 2003. Human susceptibility and resistance to Norwalk virus infection. Nat. Med. **9:**548–553.
24. **Madore, H. P., J. J. Treanor, R. Buja, and R. Dolin.** 1990. Antigenic relatedness among the Norwalk-like agents by serum antibody rises. J. Med. Virol. **32:**96–101.
25. **Mariadason, J. M., C. Nicholas, K. E. L'italien, M. Zhuang, H. J. Smartt, B. G. Heerdt, W. Yang, G. A. Corner, A. J. Wilson, L. Klampfer, D. Arango, and L. H. Augenlicht.** 2005. Gene expression profiling of intestinal epithelial cell maturation along the crypt-villus axis. Gastroenterology **128:**1081–1088.
26. **Marionneau, S., F. Airaud, N. V. Bovin, J. Le Pendu, and N. Ruvoen-Clouet.** 2005. Influence of the combined ABO, FUT2, and FUT3 polymorphism on susceptibility to Norwalk virus attachment. J. Infect. Dis. **192:**1071–1077.
27. **Marionneau, S., N. Ruvoen, B. Le Moullac-Vaidye, M. Clement, A. Cailleau-Thomas, G. Ruiz-Palacois, P. Huang, X. Jiang, and J. Le Pendu.** 2002. Norwalk virus binds to histo-blood group antigens present on gastroduodenal epithelial cells of secretor individuals. Gastroenterology **122:**1967–1977.
28. **Matson, D. O., M. K. Estes, T. Tanaka, A. V. Bartlett, and L. K. Pickering.** 1990. Asymptomatic human calicivirus infection in a day care center. Pediatr. Infect. Dis. J. **9:**190–196.
29. **Meyer, R. C., E. H. Bohl, and E. M. Kohler.** 1964. Procurement and maintenance of germ-free swine for microbiological investigations. Appl. Microbiol. **12:**295–300.
30. **Moon, H. W., E. M. Kohler, and S. C. Whipp.** 1973. Vacuolation: a function of cell age in porcine ileal absorptive cells. Lab. Investig. **28:**23–28.
31. **Morotti, R. A., S. S. Kaufman, T. M. Fishbein, N. K. Chatterjee, M. E. Fuschino, D. L. Morse, and M. S. Magid.** 2004. Calicivirus infection in pediatric small intestine transplant recipients: pathological considerations. Hum. Pathol. **35:**1236–1240.
32. **Parker, S. P., W. D. Cubitt, X. J. Jiang, and M. K. Estes.** 1994. Seroprevalence studies using a recombinant Norwalk virus protein enzyme immunoassay. J. Med. Virol. **42:**146–150.
33. **Parker, T. D., N. Kitamoto, T. Tanaka, A. M. Hutson, and M. K. Estes.** 2005. Identification of genogroup I and genogroup II broadly reactive epitopes on the norovirus capsid. J. Virol. **79:**7402–7409.
34. **Paul, P.** 1989. Production and characterization of monoclonal antibodies to porcine immunoglobulin gamma, alpha, and light chains. Am. J. Vet. Res. **50:**471–475.
35. **Pesavento, P. A., N. J. MacLachlan, L. Dillard-Telm, C. K. Grant, and K. F. Hurley.** 2004. Pathologic, immunohistochemical, and electron microscopic findings in naturally occurring virulent systemic feline calicivirus infection in cats. Vet. Pathol. **41:**257–263.
36. **Richards, G. P., M. A. Watson, R. L. Fankhauser, and S. S. Monroe.** 2004. Genogroup I and II noroviruses detected in stool samples by real-time reverse transcription-PCR using highly degenerate universal primers. Appl. Environ. Microbiol. **70:**7179–7184.
37. **Roberts, L. O., N. Al-Molawi, M. J. Carter, and G. E. Kass.** 2003. Apoptosis in cultured cells infected with feline calicivirus. Ann. N. Y. Acad. Sci. **1010:**587–590.
38. **Rockx, B., M. De Wit, H. Vennema, J. Vinje, E. De Bruin, Y. Van Duynhoven, and M. Koopmans.** 2002. Natural history of human calicivirus infection: a prospective cohort study. Clin. Infect. Dis. **35:**246–253.
39. **Rockx, B. H., W. M. Bogers, J. L. Heeney, G. van Amerongen, and M. P. Koopmans.** 2005. Experimental norovirus infections in non-human primates. J. Med. Virol. **75:**313–320.
40. **Saif, L. J., L. A. Ward, L. Yuan, B. I. Rosen, and T. L. To.** 1996. The gnotobiotic pig as a model for studies of disease pathogenesis and immunity to human rotaviruses. Arch. Virol. **12**(Suppl.)**:**153–161.
41. **Schlegel, A., T. Giddings, Jr., M. Ladinsky, and K. Kirkegaard.** 1996. Cellular origin and ultrastructure of membranes induced during poliovirus infection. J. Virol. **70:**6576–6588.
42. **Schreiber, D. S., N. R. Blacklow, and J. S. Trier.** 1974. The small intestinal lesion induced by Hawaii agent acute infectious nonbacterial gastroenteritis. J. Infect. Dis. **129:**705–709.
43. **Shoup, D. I., D. E. Swayne, D. J. Jackwood, and L. J. Saif.** 1996. Immunohistochemistry of transmissible gastroenteritis virus antigens in fixed paraffin-embedded tissues. J. Vet. Diagn. Investig. **8:**161–167.
44. **Sosnovtsev, S. V., E. A. Prikhod'ko, G. Belliot, J. I. Cohen, and K. Y. Green.** 2003. Feline calicivirus replication induces apoptosis in cultured cells. Virus Res. **94:**1–10.
45. **Subekti, D. S., P. Tjaniadi, M. Lesmana, J. McArdle, D. Iskandriati, I. N. Budiarsa, P. Walujo, I. H. Suparto, I. Winoto, J. R. Campbell, K. R. Porter, D. Sajuthi, A. A. Ansari, and B. A. Oyofo.** 2002. Experimental infection of Macaca nemestrina with a Toronto Norwalk-like virus of epidemic viral gastroenteritis. J. Med. Virol. **66:**400–406.
46. **Sugieda, M., H. Nagaoka, Y. Kakishima, T. Ohshita, S. Nakamura, and S. Nakajima.** 1998. Detection of Norwalk-like virus genes in the caecum contents of pigs. Arch. Virol. **143:**1215–1221.
47. **Sugieda, M., and S. Nakajima.** 2002. Viruses detected in the caecum contents of healthy pigs representing a new genetic cluster in genogroup II of the genus "Norwalk-like viruses." Virus Res. **87:**165–172.
48. **van Der Poel, W. H., J. Vinje, R. van Der Heide, M. I. Herrera, A. Vivo, and M. P. Koopmans.** 2000. Norwalk-like calicivirus genes in farm animals. Emerg. Infect. Dis. **6:**36–41.
49. **Wang, Q. H., K. O. Chang, M. G. Han, S. Sreevatsan, and L. J. Saif.** 2006. Development of a new microwell hybridization assay and an internal control RNA for the detection of porcine noroviruses and sapoviruses by reverse transcription-PCR. J. Virol. Methods **132:**135–145.
50. **Wang, Q. H., M. G. Han, S. Cheetham, M. Souza, J. A. Funk, and L. J. Saif.** 2005. Porcine noroviruses related to human noroviruses. Emerg. Infect. Dis. **11:**1874–1881.
51. **Ward, L. A., B. I. Rosen, L. Yuan, and L. J. Saif.** 1996. Pathogenesis of an attenuated and a virulent strain of group A human rotavirus in neonatal gnotobiotic pigs. J. Gen. Virol. **77:**1431–1441.
52. **Watson, A. J., S. Chu, L. Sieck, O. Gerasimenko, T. Bullen, F. Campbell, M. McKenna, T. Rose, and M. H. Montrose.** 2005. Epithelial barrier function in vivo is sustained despite gaps in epithelial layers. Gastroenterology **129:**902–912.
53. **Wobus, C. E., S. M. Karst, L. B. Thackray, K. O. Chang, S. V. Sosnovtsev, G. Belliot, A. Krug, J. M. Mackenzie, K. Y. Green, and H. W. Virgin.** 2004. Replication of Norovirus in cell culture reveals a tropism for dendritic cells and macrophages. PLoS Biol. **2:**e432.
54. **Wyatt, R. G., R. Dolin, N. R. Blacklow, H. L. DuPont, R. F. Buscho, T. S. Thornhill, A. Z. Kapikian, and R. M. Chanock.** 1974. Comparison of three agents of acute infectious nonbacterial gastroenteritis by cross-challenge in volunteers. J. Infect. Dis. **129:**709–714.
55. **Yuan, L., C. Iosef, M. S. Azevedo, Y. Kim, Y. Qian, A. Geyer, T. V. Nguyen, K. O. Chang, and L. J. Saif.** 2001. Protective immunity and antibody-secreting cell responses elicited by combined oral attenuated Wa human rotavirus and intranasal Wa 2/6-VLPs with mutant *Escherichia coli* heat-labile toxin in gnotobiotic pigs. J. Virol. **75:**9229–9238.
56. **Yuan, L., S. Ishida, S. Honma, J. T. Patton, D. C. Hodgins, A. Z. Kapikian, and Y. Hoshino.** 2004. Homotypic and heterotypic serum isotype-specific antibody responses to rotavirus nonstructural protein 4 and viral protein (VP) 4, VP6, and VP7 in infants who received selected live oral rotavirus vaccines. J. Infect. Dis. **189:**1833–1845.